Localization of Frontier Orbitals on Anatase Nanoparticles Impacts Water Adsorption

ARTICLE *in* THE JOURNAL OF PHYSICAL CHEMISTRY C · SEPTEMBER 2009

Impact Factor: 4.77 · DOI: 10.1021/jp905489s

2 AUTHORS:

Hong Wang
West Virginia University
24 PUBLICATIONS **734** CITATIONS
SEE PROFILE

James P Lewis
West Virginia University
90 PUBLICATIONS **2,796** CITATIONS
SEE PROFILE

Localization of Frontier Orbitals on Anatase Nanoparticles Impacts Water Adsorption

Hong Wang* and James P. Lewis

Department of Physics, West Virginia University, Morgantown, West Virginia 26506-6315

Received: June 11, 2009; Revised Manuscript Received: July 28, 2009

We present a computational investigation of spherical anatase nanoparticles with size ranging from 1.5 to 2.4 nm using density functional theory. Our results show that structural changes only occur within one or two unit cells from the surface regardless of the size of the nanoparticle. Hence, as the size of the nanoparticle increases, the effect of surface reconstruction penetrating into the interior obviously decreases and anatase nanoparticles rapibly obtain bulk-like structure for increasing size. Analysis of the nanoparticles in our work indicates that the frontier orbitals (so-called HOMOs) are mostly localized on low-coordinated Ti atoms which are located on corner positions of nanoparticles. These corner positions solely consist of 4-coordinated Ti atom lack of bridge oxygen atoms. These low-coordinated positions are the most energetically favored adsorption sites for water. The frontier orbitals located at these low-coordinated Ti sites become more localized with increased nanoparticle size resulting in increasing binding energy for water adsorption.

1. Introduction

Since Fujishima and Honda succeeded to photocatalytically cleave water into oxygen and hydrogen with a TiO_2−Pt anode−cathode system,[1] titanium dioxide has attracted extensive attention for many applications. In recent decades, as improvements have been made to synthesize nanostructures, nanoscale titanium dioxide materials have been exploited extensively in many applications including photocatalysis, solar cells, biomaterials, memory devices, and as environmental catalysts.[2−22] Among TiO_2 polymorphs, anatase is of paramount importance since it exhibits higher activity in many cases,[23] especially as the system size decreases to the nanoscale; TiO_2 nanocrystals appear to prefer the metastable anatase phase rather than the rutile phase due to the lower surface energy of anatase particles.[16]

In contrast to the extensive work reported on the electronic and atomic structure of bulk anatase and rutile, as well as of some studies on their low index surfaces,[11] understanding the corresponding nanoscale properties of TiO_2 nanomaterials is incomplete. Some studies already identify the structure of the most stable small TiO_2 aggregates; and these studies provide a starting point for further investigations on quantum size effects on photophysics, substrate−particle or particle−particle binding, and charge transfer, as well as for understanding the nucleation of larger TiO_2 particles.[24,25] Moreover, some experimental work such as EXAFS, XANES, UV−vis, and Raman spectroscopy, etc., shows an increasing presence of distorted octahedral as well as 3- and 4-fold coordinated Ti atoms as the particle size decreases.[21,26−29] These low-coordinated Ti atoms exposed on the surface of nanoparticles generally are believed to present unique adsorption properties for water oxidation with TiO_2 serving as a photocatalyst.

To gain insight into the unique photochemistry of TiO_2 nanoparticles, others have performed theoretical calculations on both cluster models and normal slab models to further understand the correlation between surface orientations and electronic properties.[12,30−32] DFT approaches are proven to be efficient and have been adopted to probe geometric and electronic structures of anatase nanoparticles. Previous work proposed that the unique surface photochemistry exhibited in anatase nanoparticles results from surface-trapped holes on unsaturated and exposed Ti/O atoms. These special surface sites serve as "hot spots" which perform oxidation (by holes) or reduction (by electrons). Additionally, thermodynamic approaches using surface edge and vertex energies to predict shapes and energetics of large nanoparticles are also reliable for determining their performance in particular applications.[33,34] Electronic structure calculations of nanoparticles are challenging as experimentally relevant nanoparticle sizes often surpass the upper limit of calculations. The detailed understanding about chemical processes occurring at the surface of larger and larger nanoparticles requires more thorough investigation.

In our present work, we perform ab initio tight-binding calculations on a series of anatase nanoparticles which range in size from 1.5 to 2.4 nm. We demonstrate the atomic structures and electronic properties of these medium size anatase nanoparticles, as well as interpret the underlying mechanisms of the chemical processes of water molecule adsorption on different sites on the surface of anatase nanoparticles. Our detailed study provides solid evidence that the geometric and electronic properties of nanoparticles are very different from those of bulk anatase. Generally, it is believed that the behavior of TiO_2 nanoparticles is greatly different from that of either bulk or atomic scale clusters due to the formation of disordered curvature of the facets exposed in nanoparticles. The surface energies of finite size particles are different from the surface energies of planar surfaces, as the curvature of the finite size particles must be accounted for in addition to their shape. Therefore, critical questions to be addressed to complete our understanding of unique photoactivity presented in anatase nanoparticles include (1) how the ratio of surface to volume affects the geometric structures and electronic properties of anatase nanoparticles and (2) how the unsaturated Ti atoms and O atoms exposed on the surface of the particles enhance the chemical activity to attract the small molecules to adsorb on some locations of the particles.

* To whom correspondence should be addressed. E-mail: hong.wang@mail.wvu.edu.

10.1021/jp905489s CCC: $40.75
Published on Web 08/28/2009

TABLE 1: Anatase Unit Cell Parameters

volume ($Å^3/TiO_2$)	34.54
lattice constant a (Å)	3.797
lattice constant b (Å)	9.575
internal parameter u	0.208

The paper is organized as follows: In Section 2, the computational method used in this work is described, including a brief introduction of the FIREBALL DFT code. The geometric structures after optimization are discussed in Section 3.1, which is followed by the electronic properties analysis in Section 3.2. Finally, the implication of our theoretical results for water adsorption on nanoparticle surfaces is examined in Section 3.3. In Section 4, the main conclusion is summarized.

2. Computational Approach

In this work, we carry out the calculations of chosen anatase nanoparticles using an ab initio tight-binding method, called FIREBALL, which is a self-consistent electronic structure code based on the local density approximation[35,36] of density-functional theory (DFT) with a nonlocal pseudopotential scheme.[37] This method has been successfully applied to a number of systems such as zeolites, clathrate structures, semiconducting materials, and biomolecules.[37−41] A brief description of the method will be given here, and we recommend the reader see ref 37 and references therein for detailed instructions of the method. In this work, we chose a minimal basis set for Ti (r_c = 6.3, 6.0, 5.7), O (r_c = 3.6, 4.1), and H (r_c = 3.8), as well as adding a $4p^0$ state to the Ti ground state for polarization. The r_c values in parentheses are the cutoff of the wave functions (in atomic units) for s, p, and d shells, respectively.

Previous work on bulk TiO_2 material demonstrates that FIREBALL is able to correctly predict the accurate electronic properties of the TiO_2 system.[42] For constructing and predicting the atomic and electronic structures of the anatase nanoparticles, we first examined our previous calculations on the geometric and electronic structure of bulk anatase, which belongs to the space group $I4_1/amd$ (D_{4h}^{19}) and contains 12 atoms per conventional unit cell.[43] (Lattice parameters are shown in Table 1.) On the basis of the unit cell of bulk anatase, we construct the anatase nanoparticles with diameters ranging from 1.5 to 2.4 nm, as shown in Figure 1. These nanoparticles are generated spherically from a Ti centered atom with no bias to specific facets. Our choice in nanoparticles provides a rich diversity in unsaturated Ti/O atoms with dangling bonds existing at the surfaces of these nanoparticles; such diversity will greatly affect the electronic structures.

Figure 1 shows the snapshots of the final configurations of the nanoparticles after optimization. We use a simple quenching minimization algorithm to optimize the nanoparticle structures and no special annealing simulations were performed as we wish to preserve the anatase phase. In all cases, some of the surface oxygen ions or titanium ions were removed to ensure electroneutrality. Additionally, stoichiometry is presented, keeping the ratio of Ti atoms and O atoms at 1:2, yielding a mix of 5-, 4-, and 3-coordinated Ti atoms and singly coordinated O atoms exposed on the facets of spherical nanoparticles. Different from structural properties of fully coordinated Ti in stable planar surfaces, nanoparticle facets yield 3- and 4-coordinated Ti atoms. These low-coordinated Ti atoms on anatase nanoparticles were observed in experimental work and are considered to produce the unique surface photochemistry found in nanoparticles.[44,45] The fraction of surface atoms increases as the size of nanoparticles decreases, leading to a greater variety in bond lengths and bond angles. Thus, we define the geometry coordination numbers of the Ti atoms in the optimized anatase nanoparticles by examining any oxygen ion with a bond length shorter than 2.3 Å to the low-coordinated Ti atoms.

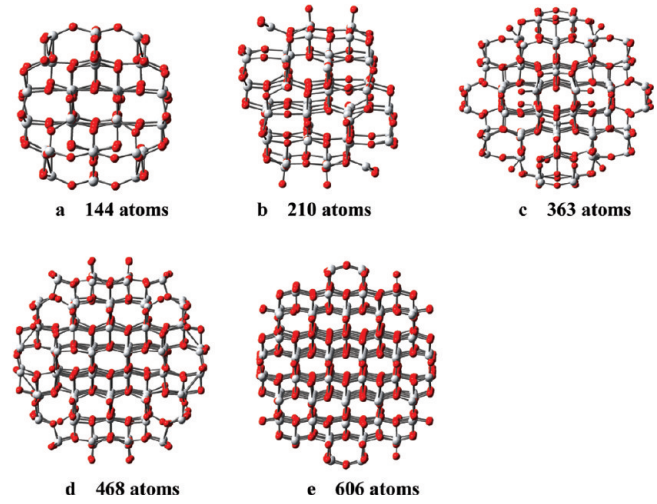

Figure 1. Snapshots of optimized nanoparticles for 144 to 606 atoms (1.5 to 2.4 nm).

3. Results and Discussion

3.1. Initial Configurations and Relaxed Structures. As shown in Figure 1, the atoms at the surface of each nanoparticle present significant structural disorder compared to the initial bulk geometries, especially for the smallest particle with 144 atoms. On the basis of the optimized structures, we are able to observe that both the Ti atoms and O atoms of the surface show significant structural disorder, which is mainly displayed in the change of Ti−O bond lengths on the surfaces. However, for the smallest particle $(TiO_2)_{48}$ with 144 atoms, the structural disorder is not only limited to the surface atoms, but also there is significant interior Ti−O reconstruction in the Ti−O bonds, as shown in isomer **a**. Similar structural changes can be traced in the 210 atom and 363 atom nanoparticles, as shown in **b** and **c** in Figure 1. But as size increases, fewer structural changes occur in larger nanoparticles than in smaller nanoparticles, which is shown in 468 atoms and 606 atoms nanoparticles as isomers **d** and **e** in Figure 2.

As indicated in structure **1a**, we find that the oxygen atoms on the surface move outward, while the titanium atoms tend to move inward, resulting in a few low-coordinated Ti atoms exposed at the nanoparticle surface. This significant surface reordering to reduce the surface tension is consistent with previous observations in experiments and molecular dynamic simulations.[21,46] For the nanoparticle with 144 atoms, the bond length for the Ti−O bonds is shortened from the original value of 1.97 Å to 1.85 Å for most of the 4-coordinated Ti atoms in the surface; however, even the bond length of the Ti−O bond for the 6-coordinated Ti atoms in the interior shows changes. One of the six Ti−O bonds becomes extremely longer (2.21 Å) than the original Ti−O bond length, while the other five bond lengths are close to 1.98 Å. We also observe the same structural disorder trends for the 6-coordinated Ti atoms near the surface layers in nanoparticles containing 210 and 368 atoms. As the size of the nanoparticles continuously increases, the structural disorder presented at the interior tends to decrease as the proportion of surface decreases. For the larger nanoparticles (468 atoms and 606 atoms), only the bond length of Ti−O bonds

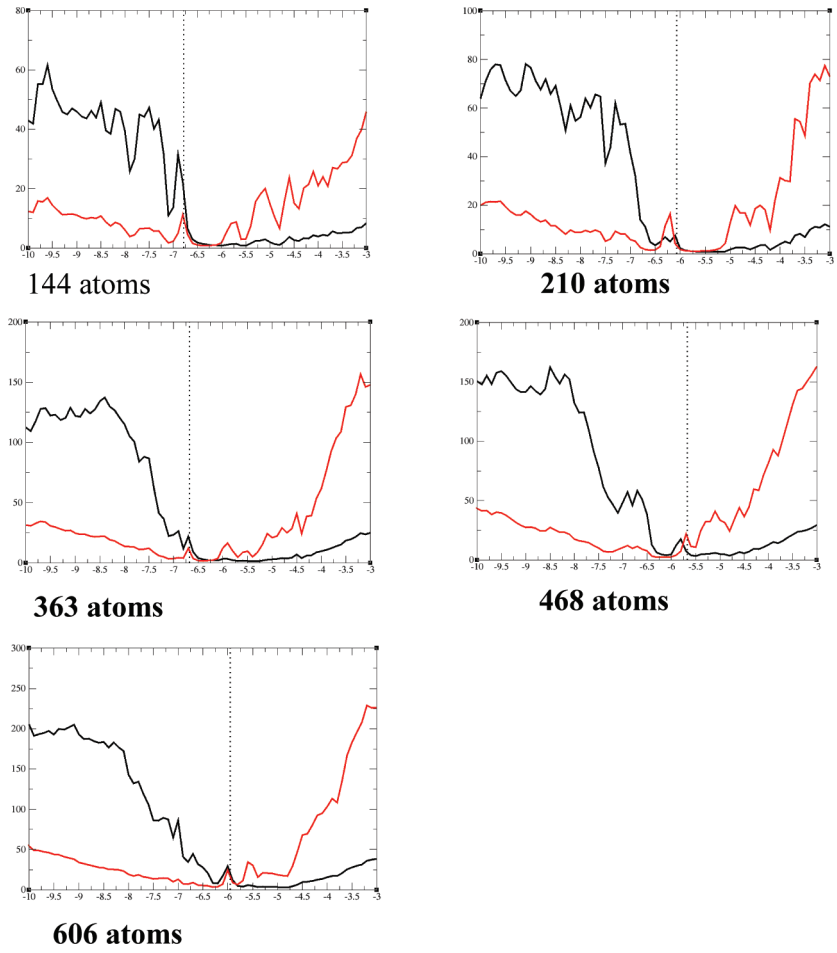

Figure 2. The bond length distribution in optimized nanoparticles 144 atoms−606 atoms. The small window is the bond distribution for the anatase nanoparticles before optimization.

in the surfaces (one monolayer) shows obvious changing due to lower coordination.

3.2. Electronic Properties: Surface States and Frontier Orbitals. As TiO_2 is one of the most important materials for photocatalyst applications, it is important to investigate how the structural changes of optimized anatase nanoparticles affect the electronic properties, which are greatly influenced by the high surface-to-bulk ratio found in nanoparticles. More interestingly, there are many corner or edged Ti atoms with low coordination exposed on the nanoparticle surface that can play an important role for the surface chemistry of nanoparticles.[11,12,47−49] Thus, the correlation between special low-coordinated "corner" Ti atoms and the corresponding unique electronic properties is significant for understanding the special photocatalytic activity of nanoparticles. Due to the quantum size effect, the energy gap of nanoparticles is much larger than the band gap of bulk anatase. As shown in Figure 2, the energy gaps for all nanoparticles range from 3.5 eV for the largest nanoparticle we examined to 4.5 eV for the smallest. Although wider energy gaps of anatase nanoparticles appear to lack promise for photocatalytic reactions, the unique appearance exhibited in their electron density of states (DOS) plots may yield unexpected active performance.

In Figure 2, we plot the partial density of states (PDOS) corresponding to Ti atoms and O atoms in the chosen nanoparticles and compare these PDOS to the total DOS. The primary point about the nanoparticles' PDOS is that we find that the states existing between the valence band and the conduction band are entirely due to the low-coordinated Ti atoms at the surface. The finding of surface states in the gap is similar to previous experimental and computational work on bulk anatase.[50−52] In our work, we find that Ti 3d states not only define the conduction band but also show a peak near the valence band. With increasing particle size, these Ti 3d surface states shift toward the conduction band and decrease in amplitude. Therefore, we contend that these peaks are produced from the 3-coordinated Ti atoms mostly distributed in the corner position at the nanoparticle surface. However, the fraction of 3-coordinated Ti atoms decreases along with increasing nanoparticle size, leading to a higher active adsorption area exposed to the species around the larger nanoparticles.

In addition to the PDOS, we examine the frontier orbitals of these nanoparticles and we further depict the frontier molecular orbitals which we believe are mainly responsible for the fundamental optoelectronic properties when titanium dioxide nanoparticles are applied in photoelectrochemistry and photocatalysis. Due to nanoparticle pseudosymmetry, there are several energy levels which near the Fermi level are equivalent in energy, to some extent. These frontier orbitals are localized at similar geometric positions, as seen in Figure 5, and are mostly located at corner sites of the surface, thus these frontier states correspond to low-coordinated Ti atoms. These corner Ti atoms are connected by so-called bridge oxygen atoms which are the basic structural character of the (001) anatase surface, which is proposed to be more reactive but less stable in anatase facets.[23]

To verify how these frontier orbitals distribute on the nanoparticle surfaces, we define the degree of localization by *W*, which gives the number of accessible atoms in a particular

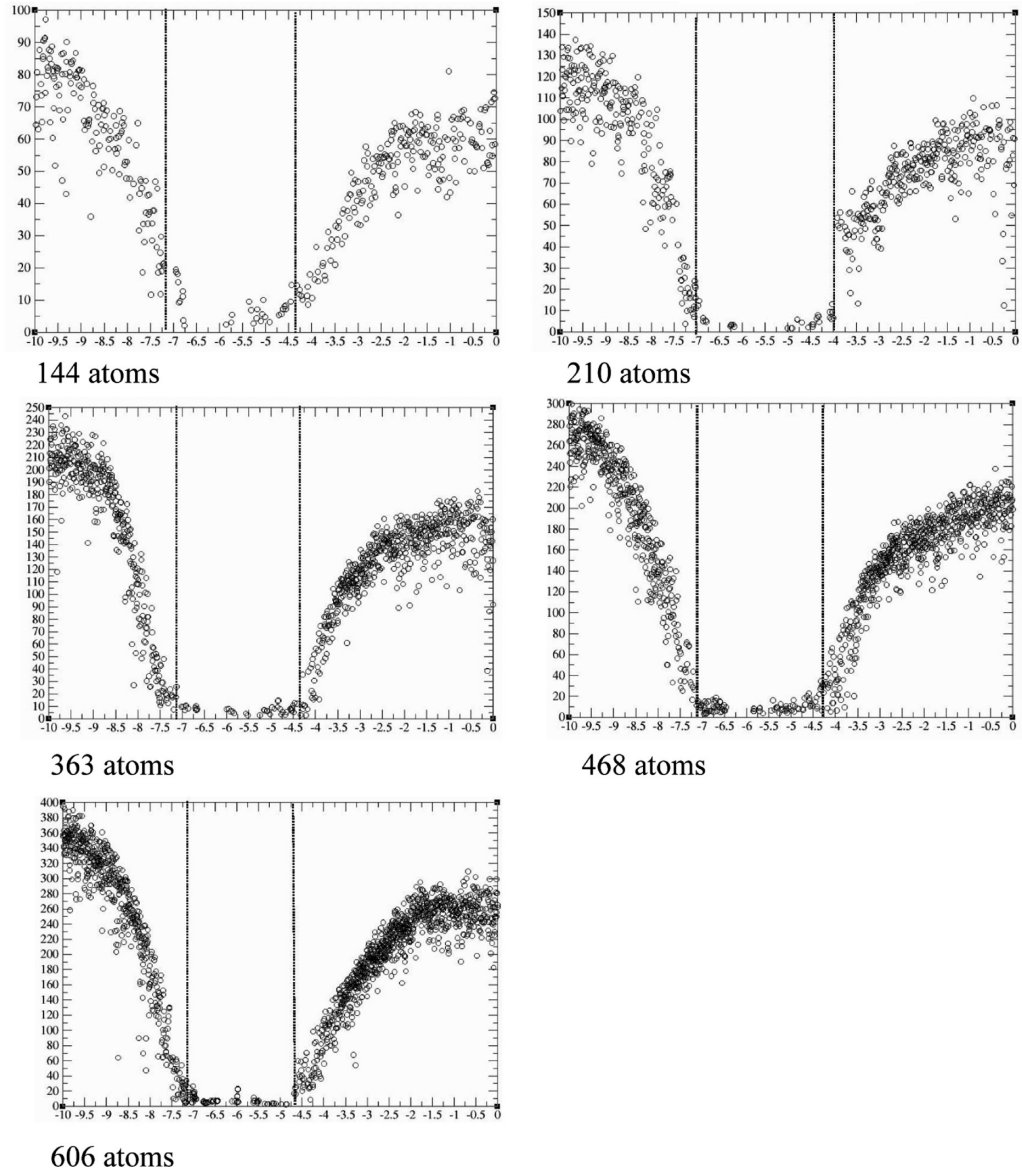

Figure 3. The PDOS of nanoparticles 144 atoms to 606 atoms. (Black curves represent O atoms density of states, while red curves represent Ti atoms density of states. The dash lines are the edge energy of the valence band and the conduction band.)

electronic state (v) and describes the spatial extent of this state. The details about W and $W(v)$ with can be found in ref 42. As shown in Figure 3, there are some very localized states existing between valence band and conduction band. These localized states are distributed on a few atoms, which is obvious in both Figures 2 and 3. More interestingly, these frontier orbitals, which mostly occur near the edge of valence band, are *more localized* for *increasing* nanoparticle size. These highly localized surface states result from the low-coordinated Ti atoms on the surface which can also be viewed as surface defects. Therefore, the states from these surface defects are isolated from other electronic states and do not mix greatly; this mixing is even smaller as the nanoparticle increases in size. This behavior is similar to what is observed when donor states are found midgap and thus isolated from the valence band and conduction bands.

We project the frontier orbitals onto the nanoparticle structure as shown in Figure 4. As predicted from the PDOS, we find that these frontier orbitals are mostly located on the surface of nanoparticles at the low-coordinated Ti atoms exposed in the surfaces. The frontier orbitals in Figure 4 indicate that these surface states located on the low-coordinated Ti atoms are also more localized with increasing nanoparticle size as predicted by our calculations of W in Figure 3. For the largest nanoparticle with 606 atoms, the HOMOs become more localized and exclusively on Ti atoms, which may explain why the reactivity becomes obvious in these low-coordinated Ti corner sites when nanoparticles become larger.

3.3. Water Adsorption on the Nanoparticle and the Favorite Adsorption Sites. It is well accepted that the disorder structures and distinct electronic properties of titanium oxide nanoparticles distinguish anatase nanoparticles from larger bulk materials.[21,33] These unique properties also result in their extraordinary surface adsorption chemical reactions happening in nanoparticles' surfaces which made nanoparticle surface chemistry attract more attention in the past decade.[49] For nanoparticles, the surface−volume ratio is a very important fact accounting for the unique surface chemistry activities happening in nanoparticles. In other words, there are many low-coordinated Ti atoms exposing outside and present interesting adsorption properties for water adsorption. These low-coordinated Ti atoms are even lower coordinated that 5-coordinated Ti arranged on an anatase (001) surface. As we previously discussed, the

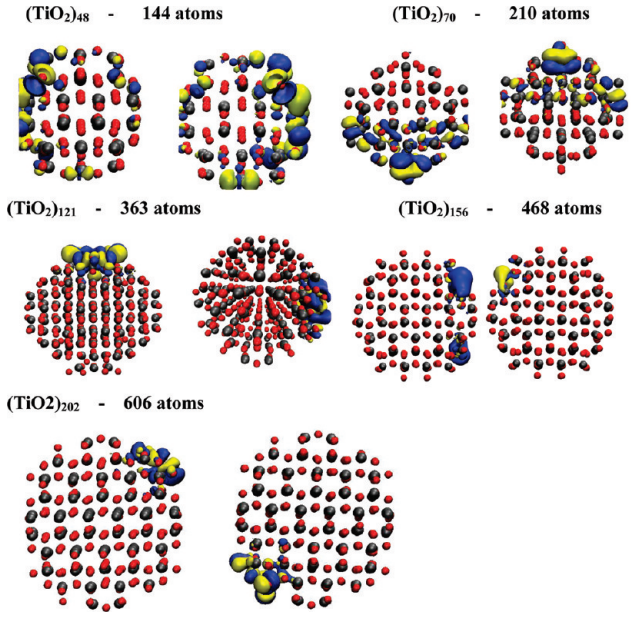

Figure 4. The frontier molecular orbitles of anatase nanoparticles.

frontier orbitals are mostly located in these low-coordinated Ti atoms around corner or edge sites. Thus, we added a water molecule at different sites on the optimized anantase nanoparticle surfaces to determine the best adsorption sites.

On the basis of the analysis of the frontier orbitals and PDOS of nanoparticles, there are several adsorption sites for water adsorption under consideration in order to compare the adsorption ability between the chosen adsorption sites. As shown in Figure 5, we chose three different adsorption sites which represent the corner-edge sites and planar sites at the surface. Corresponding to the locations where the frontier orbitals are located, the corner-edge sites, for example, the site **1a** in Figure 5, on the surface correspond to the site where the frontier orbitals are mostly localized. At each site, we calculate the total binding energy for comparing the adsorption abilities at each site according to E(nanoparticle) + E(water) − E(total system). We find that this binding energy increases with increasing nanoparticle size with the difference in binding energy decreasing with increasing size (the binding energy is converging to a specific value).

Also, it should be mentioned that the site **a** listed here is not the only stable adsorption site for water. For these spherically shaped nanoparticles, there are several low-coordinated corner or edge sites exposed on the surface. Thus, we further investigated whether these other low-coordinated sites are more or less attractive for water adsorption. We performed a comparison between one typical very low-coordinated site (3- or 4-coordinated) with two other sites for each nanoparticle instead of listing all the low-coordinated sites for each nanoparticle. Interestingly, for all these selected adsorption sites, the sites with the lowest coordinated Ti atoms at the corner sites show greater attraction for water adsorption. The adsorption energy for sites **a** is at least 0.88 eV lower than the energy of other sites we tested in this work, corresponding to different nanoparticle sizes.

The relative adsorption energies of sites **b** and **c** are also shown under the structures in Figure 5. The bond length between the Ti atom and the O atom of H_2O in each **a** configuration is 2.03 Å, which is slightly longer than the equatorial Ti−O bond length of anatase. However, the H−O bond length was also found to be 1.11 Å, which is also slightly longer than the O−H

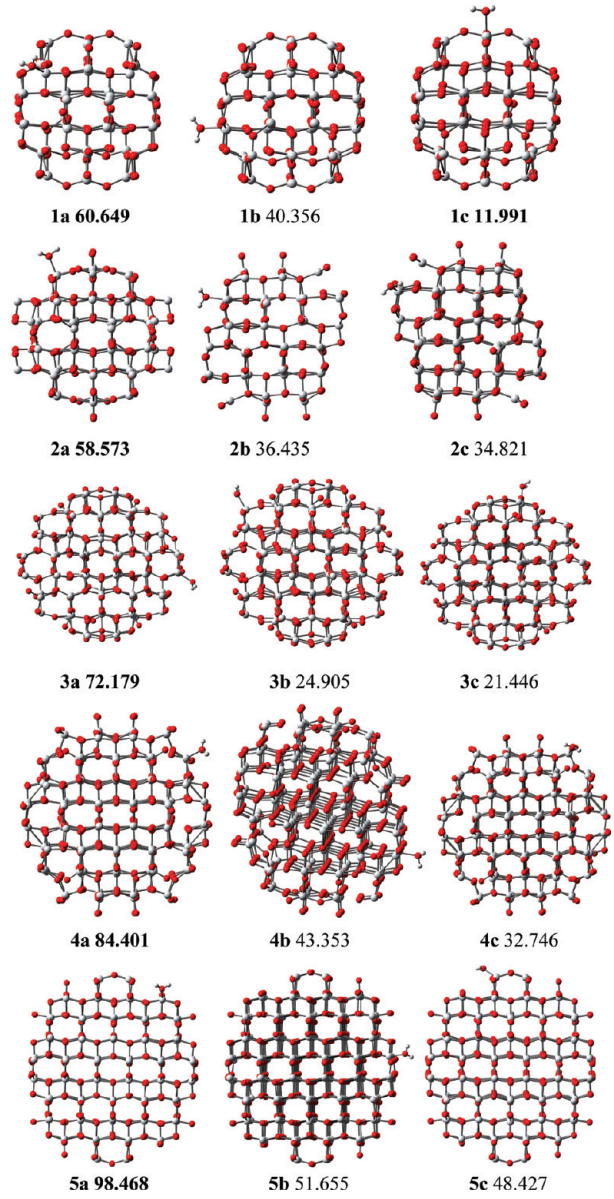

Figure 5. Water adsorption on a, b, and c sites on nanoparticles 144 to 606 atoms. (The relative adsorption energy shown under the structures is the cohesive energy difference between site a and b (c). We set the first sites **a** with 0.0 eV.)

bond length in water. All of this is certainly confirmed by the analysis of the frontier molecular orbitals presented in Section 3.2; it is interesting to note that the favorable adsorption positions for the water molecule on these nanoparticles are at the exact the same locations where the frontier orbitals (so-called HOMOs) are the most localized in each configuration. Thus, localized frontier orbitals present strong attraction for the water molecules existing in the environment and likely act like active spots for the external molecules adsorption. And we firmly conclude, as proposed by Fukui,[53] the frontier orbitals which are more localized in larger nanoparticles yield increased water adsorption on these corner, low-coordinated Ti atoms.

4. Conclusion

In summary, we presented results of ab initio DFT simulation on anatase nanoparticles with a size ranging from 1.5 to 2.4 nm. Applying FIREBALL computational code, which adopted a slightly excited basis set for the atoms of

the system, we are able to utilize our DFT calculations from small clusters to nanoscale size particles with at least more than 100 atoms. The relaxed structures show that the portion of surface in the whole structure affects the geometric configuration of anatase nanoparticles. The amount of surface reconstruction remains constant to only the first or second monolayers regardless of nanoparticle size. Further analysis of the frontier orbitals indicates that the corner positions, consisting of 3- or 4-coordinated Ti atoms lacking bridge oxygen atoms, are the most reactive. As we adsorb water molecules on different positions on the facets of nanoparticles optimized in our work, we find that these localized frontier orbital sites are the most energetically conducive to water adsorption. This localization increases with increasing nanoparticle size and thus also creates more tightly bound water adsorption sites with increasing nanoparticle size. These special corner positions are thus "hot spots" for molecular adsorption existing in the nanoparticles' environment.

Acknowledgment. This work was funded largely by the NSF (EPS 0554328) with matching funds from the West Virginia University Research Corporation and the West Virginia EPSCoR Office and in part by a subcontract (No. 41817M2187/41817M2100) from Research and Development Solutions, LLC under contract from the Department of Energy's National Energy Technology Laboratory. Computational facilities and resources used in this work are also supported by EPS 0554328 (with matching funds from the West Virginia University Research Corporation and the West Virginia EPSCoR Office). We would also like to thank Prof. Juliana Boerio-Goates at Brigham Young University for helpful discussions on this research.

References and Notes

(1) Fujishima, A.; Honda, K. Electrochemical Photolysis of Water at a Semiconductor Electrode. *Nature* **1972**, *238* (5358), 37–38.

(2) Liu, G. H.; et al. Destructive adsorption of carbon tetrachloride on nanometer titanium dioxide. *Phys. Chem. Chem. Phys.* **2004**, *6* (5), 985–991.

(3) Nakamura, R.; et al. In situ FTIR studies of primary intermediates of photocatalytic reactions on nanocrystalline TiO_2 films in contact with aqueous solutions. *J. Am. Chem. Soc.* **2003**, *125* (24), 7443–7450.

(4) Tan, B.; Wu, Y. Y. Dye-sensitized solar cells based on anatase TiO_2 nanoparticle/nanowire composites. *J. Phys. Chem. B* **2006**, *110* (32), 15932–15938.

(5) Oregan, B.; Gratzel, M. A Low-Cost, High-Efficiency Solar-Cell Based on Dye-Sensitized Colloidal TiO_2 Films. *Nature* **1991**, *353* (6346), 737–740.

(6) Zhang, H. Z.; et al. Enhanced adsorption of molecules on surfaces of nanocrystalline particles. *J. Phys. Chem. B* **1999**, *103* (22), 4656–4662.

(7) Wang, C. Y.; Groenzin, H.; Shultz, M. J. Comparative study of acetic acid, methanol, and water adsorbed on anatase TiO_2 probed by sum frequency generation spectroscopy. *J. Am. Chem. Soc.* **2005**, *127* (27), 9736–9744.

(8) Martyanov, I. N.; et al. Structural defects cause TiO_2-based photocatalysts to be active in visible light. *Chem. Commun.* **2004**, (21), 2476–2477.

(9) Martin, S. T.; et al. Surface structures of 4-chlorocatechol adsorbed on titanium dioxide. *Environ. Sci. Technol.* **1996**, *30* (8), 2535–2542.

(10) Chen, X.; Mao, S. S. Titanium dioxide nanomaterials: Synthesis, properties, modifications, and applications. *Chem. Rev.* **2007**, *107* (7), 2891–2959.

(11) Diebold, U. The surface science of titanium dioxide. *Surf. Sci. Rep.* **2003**, *48* (5−8), 53–229.

(12) Gong, X. Q.; Selloni, A.; Vittadini, A. Density functional theory study of formic acid adsorption on anatase TiO_2(001): Geometries, energetics, and effects of coverage, hydration, and reconstruction. *J. Phys. Chem. B* **2006**, *110* (6), 2804–2811.

(13) Lu, H. M.; Wen, Z.; Jiang, Q. Size dependent adsorption on nanocrystal surfaces. *Chem. Phys.* **2005**, *309* (2−3), 303–307.

(14) Elder, S. H.; et al. The discovery and study of nanocrystalline TiO_2-(MoO_3) core-shell materials. *J. Am. Chem. Soc.* **2000**, *122* (21), 5138–5146.

(15) Gribb, A. A.; Banfield, J. F. Particle size effects on transformation kinetics and phase stability in nanocrystalline TiO_2. *Am. Mineral.* **1997**, *82* (7−8), 717–728.

(16) Zhang, H. Z.; Banfield, J. F. Thermodynamic analysis of phase stability of nanocrystalline titania. *J. Mater. Chem.* **1998**, *8* (9), 2073–2076.

(17) Zhang, W. F.; et al. Photoluminescence in anatase titanium dioxide nanocrystals. *Appl. Phys. B: Lasers Opt.* **2000**, *70* (2), 261–265.

(18) Hagfeldt, A.; Gratzel, M. Light-Induced Redox Reactions in Nanocrystalline Systems. *Chem. Rev.* **1995**, *95* (1), 49–68.

(19) Einaga, H.; Futamura, S.; Ibusuki, T. Photocatalytic decomposition of benzene over TiO_2 in a humidified airstream. *Phys. Chem. Chem. Phys.* **1999**, *1* (20), 4903–4908.

(20) Kaneko, M.; Okura I. *Photocatalysis: science and technology*, Biological and medical physics series; Springer: New York, 2002; Vol. xvi, p 356.

(21) Rajh, T.; et al. Surface restructuring of nanoparticles: An efficient route for ligand-metal oxide crosstalk. *J. Phys. Chem. B* **2002**, *106* (41), 10543–10552.

(22) Vega-Arroyo, M.; et al. Quantum chemical study of TiO_2/dopamine-DNA triads. *Chem. Phys.* **2007**, *339* (1−3), 164–172.

(23) Selloni, A. Crystal growth—anatase shows its reactive side. *Nat. Mater.* **2008**, *7* (8), 613–615.

(24) Persson, P.; Gebhardt, J. C. M.; Lunell, S. The smallest possible nanocrystals of semiionic oxides. *J. Phys. Chem. B* **2003**, *107* (15), 3336–3339.

(25) Hamad, S.; et al. Structure and stability of small TiO_2 nanoparticles. *J. Phys. Chem. B* **2005**, *109* (33), 15741–15748.

(26) Chen, L. X.; et al. XAFS studies of surface structures of TiO_2 nanoparticles and photocatalytic reduction of metal ions. *J. Phys. Chem. B* **1997**, *101* (50), 10688–10697.

(27) Yeung, K. L.; et al. Ensemble effects in nanostructured TiO_2 used in the gas-phase photooxidation of trichloroethylene. *J. Phys. Chem. B* **2002**, *106* (18), 4608–4616.

(28) Grubert, G.; et al. Titanium oxide species in molecular sieves: Materials for the optical sensing of reductive gas atmospheres. *Chem. Mater.* **2002**, *14* (6), 2458–2466.

(29) Choi, H. C.; Jung, Y. M.; Kim, S. B. Size effects in the Raman spectra of TiO_2 nanoparticles. *Vib. Spectrosc.* **2005**, *37* (1), 33–38.

(30) Gong, X. Q.; Selloni, A. Reactivity of anatase TiO_2 nanoparticles: The role of the minority (001) surface. *J. Phys. Chem. B* **2005**, *109* (42), 19560–19562.

(31) Qu, Z. W.; Kroes, G. J. Theoretical study of the electronic structure and stability of titanium dioxide clusters $(TiO_2)_n$ with $n = 1-9$. *J. Phys. Chem. B* **2006**, *110* (18), 8998–9007.

(32) Qu, Z. W.; Kroes, G. J. Theoretical study of stable, defect-free $(TiO_2)_n$ nanoparticles with $n = 10-16$. *J. Phys. Chem. C* **2007**, *111* (45), 16808–16817.

(33) Barnard, A. S.; Zapol, P.; Curtiss, L. A. Modeling the morphology and phase stability of TiO_2 nanocrystals in water. *J. Chem. Theory Comput.* **2005**, *1* (1), 107–116.

(34) Barnard, A. S.; et al. Modeling the structure and electronic properties of TiO_2 nanoparticles. *Phys. Rev. B* **2006**, *73* (20), 205405.

(35) Perdew, J. P.; Zunger, A. Self-Interaction Correction to Density-Functional Approximations for Many-Electron Systems. *Phys. Rev. B* **1981**, *23* (10), 5048–5079.

(36) Perdew, J. P.; Wang, Y. Accurate and Simple Analytic Representation of the Electron-Gas Correlation-Energy. *Phys. Rev. B* **1992**, *45* (23), 13244–13249.

(37) Lewis, J. P.; et al. Further developments in the local-orbital density-functional-theory tight-binding method. *Phys. Rev. B* **2001**, *64* (19), 195103.

(38) Adams, G. B.; et al. Wide-Band-Gap Si in Open Fourfold-Coordinated Clathrate Structures. *Phys. Rev. B* **1994**, *49* (12), 8048–8053.

(39) Demkov, A. A.; et al. Electronic-Structure Approach for Complex Silicas. *Phys. Rev. B* **1995**, *52* (3), 1618–1630.

(40) Sankey, O. F.; et al. The application of approximate density functionals to complex systems. *Int. J. Quantum Chem.* **1998**, *69* (3), 327–340.

(41) Wang, H.; Lewis J. P.; Sankey O. F. Band-gap tunneling states in DNA. *Phys. Rev. Lett.* **2004**, *93* (1), 016401.

(42) Wang, H.; Lewis, J. P. Second-generation photocatalytic materials: anion-doped TiO_2. *J. Phys.: Condens. Matter* **2006**, *18* (2), 421–434.

(43) Chung, S. J.; Hahn, T.; Klee, W. E. Nomenclature and Production of 3-Periodic Lattices—the Vector Method. *Z. Kristallogr.* **1983**, *162* (1−4), 51–53.

(44) Yeredla, R. R.; Xu H. F. An investigation of nanostructured rutile and anatase plates for improving the photosplitting of water. *Nanotechnology* **2008**, *19* (5), 055706.

(45) Mogilevsky, G.; et al. Layered nanostructures of delaminated anatase: Nanosheets and nanotubes. *J. Phys. Chem. C* **2008**, *112* (9), 3239–3246.

(46) Naicker, P. K.; et al. Characterization of titanium dioxide nanoparticles using molecular dynamics simulations. *J. Phys. Chem. B* **2005**, *109* (32), 15243–15249.

(47) Barnard, A. S.; Zapol P. Effects of particle morphology and surface hydrogenation on the phase stability of TiO_2. *Phys. Rev. B* **2004**, *70* (23), 235403.

(48) Saponjic, Z. V. Shaping nanometer-scale architecture through surface chemistry. *Adv. Mater.* **2005**, *17* (8), 965–971.

(49) Grassian, V. H. When Size Really Matters: Size-Dependent Properties and Surface Chemistry of Metal and Metal Oxide Nanoparticles in Gas and Liquid Phase Environments. *J. Phys. Chem. C* **2008**, *112* (47), 18303–18313.

(50) Kurtz, R. L.; et al. Synchrotron Radiation Studies of H_2O Adsorption on TiO_2(110). *Surf. Sci.* **1989**, *218* (1), 178–200.

(51) Finazzi, E.; et al. Excess electron states in reduced bulk anatase TiO_2: Comparison of standard GGA, GGA plus U, and hybrid DFT calculations. *J. Chem. Phys.* **2008**, *129* (15), 154113.

(52) Henderson, M. A.; et al. Insights into photoexcited electron scavenging processes on TiO_2 obtained from studies of the reaction of O_2 with OH groups adsorbed at electronic defects on TiO_2(110). *J. Phys. Chem. B* **2003**, *107* (2), 534–545.

(53) Fukui, K. Chemical-Reactivity Theory—Its Pragmatism and Beyond. *Pure Appl. Chem.* **1982**, *54* (10), 1825–1836.

JP905489S